NATIONAL RENEWABLE ENERGY LABORATORY

Acceptance Performance Test Guideline for Utility Scale Parabolic Trough and Other CSP Solar Thermal Systems

Preprint

Mark S. Mehos and Michael J. Wagner
National Renewable Energy Laboratory

David W. Kearney
Kearney & Associates

To be presented at SolarPACES 2011
Granada, Spain
September 20-23, 2011

NREL is a national laboratory of the U.S. Department of Energy, Office of Energy Efficiency & Renewable Energy, operated by the Alliance for Sustainable Energy, LLC.

Conference Paper
NREL/CP-5500-52467
August 2011

Contract No. DE-AC36-08GO28308

Available electronically at http://www.osti.gov/bridge

Available for a processing fee to U.S. Department of Energy
and its contractors, in paper, from:

U.S. Department of Energy
Office of Scientific and Technical Information

P.O. Box 62
Oak Ridge, TN 37831-0062
phone: 865.576.8401
fax: 865.576.5728
email: mailto:reports@adonis.osti.gov

Available for sale to the public, in paper, from:

U.S. Department of Commerce
National Technical Information Service
5285 Port Royal Road
Springfield, VA 22161
phone: 800.553.6847
fax: 703.605.6900
email: orders@ntis.fedworld.gov
online ordering: http://www.ntis.gov/help/ordermethods.aspx

Cover Photos: (left to right) PIX 16416, PIX 17423, PIX 16560, PIX 17613, PIX 17436, PIX 17721

Printed on paper containing at least 50% wastepaper, including 10% post consumer waste.

ACCEPTANCE PERFORMANCE TEST GUIDELINE FOR UTILITY SCALE PARABOLIC TROUGH AND OTHER CSP SOLAR THERMAL SYSTEMS

Mark S. Mehos[1], Michael J. Wagner[2], and David W. Kearney[3]

[1]Program Manager, Concentrating Solar Power, National Renewable Energy Laboratory (NREL), 1617 Cole Blvd., Golden, CO 80401, USA (303) 384-7458, Mark.Mehos@nrel.gov

[2]Mechanical Engineer, National Renewable Energy Laboratory (NREL),
1617 Cole Blvd., Golden, CO 80401 (303) 384-7430

[3]Principal, PhD, Kearney & Assoc., 12804 Ober Beach Rd, Vashon WA 98070, USA, (206) 910-3851

Abstract

Prior to commercial operation, large solar systems in utility-size power plants need to pass a performance acceptance test conducted by the engineering, procurement, and construction (EPC) contractor or owners. In lieu of the present absence of ASME or other international test codes developed for this purpose, the National Renewable Energy Laboratory has undertaken the development of interim guidelines to provide recommendations for test procedures that can yield results of a high level of accuracy consistent with good engineering knowledge and practice. Progress on interim guidelines was presented at SolarPACES 2010. Significant additions and modifications were made to the guidelines since that time, resulting in a final report published by NREL in April 2011. This paper summarizes those changes, which emphasize criteria for assuring thermal equilibrium and steady state conditions within the solar field. These criteria were derived using NREL's Solar Advisor Model (SAM), which was modified to run at 5-second time steps to adequately capture the transient effects of changes in solar field inlet conditions. In addition to SAM, a model was developed that describes the time lag present between the observed delivered energy and instantaneous operating conditions. This time lag can result in a mismatch between the measured delivered energy and the delivered energy predicted by a solar field performance model.

1. Introduction

In May 2011 NREL published guidelines that provide recommendations for performance acceptance test procedures for utility-scale parabolic trough solar fields with an emphasis on thoroughly understanding the uncertainty associated with the test results [1]. The scope of the performance acceptance test guidelines is restricted to the solar field and heat transfer fluid (HTF) system as described in Fig. 1 below.

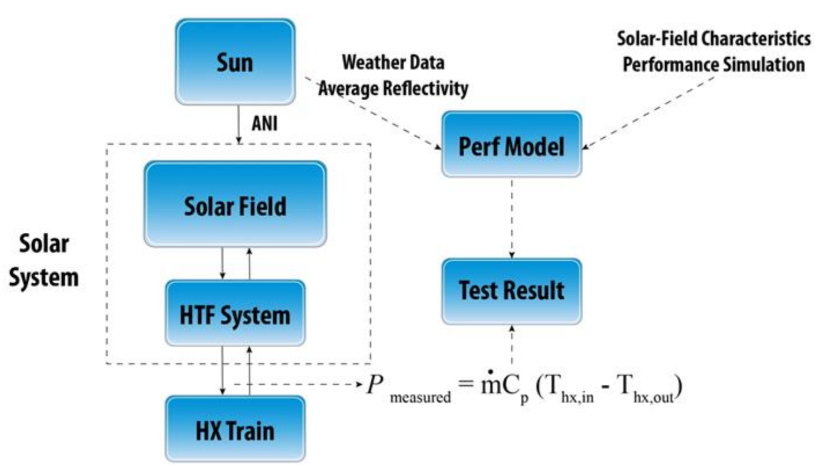

Figure 1. Schematic of Solar System Boundary

While the interim guidelines released in 2010 described the methodology for determining the uncertainty of data collected from a short term performance test [2], subsequent internal NREL discussions and review by a community of stakeholders, including the SolarPACES Task I members, identified the need for more quantitative description of the impact of variations in test conditions on the uncertainty and thermal stability, including the solar field inlet temperature, incident solar radiation, and ambient weather conditions.

2. Description of Short-Term Steady-State Tests

Test Objectives: The objective of the short duration steady-state tests is to accurately measure both the solar field power (capacity) and efficiency based on a series of tests run under clear sky conditions. The thermal power delivered from the solar field is computed from:

$$P_{measured} = \dot{m}\mathrm{C_p}\left(\mathrm{T_{hx,in}} - \mathrm{T_{hx,out}}\right) \qquad (1)$$

where $\mathrm{P_{measured}}$ is the calculated solar thermal power, $\dot{m}$ is the HTF mass flow rate, $\mathrm{C_p}$ is the temperature weighted specific heat of the heat transfer fluid (HTF), $\mathrm{T_{hx,in}}$ is the HTF average bulk inlet temperature to solar heat exchanger train, and $\mathrm{T_{hx,out}}$ is the HTF average bulk outlet temperature at the exit of the solar heat exchanger train (also at the inlet of the tough solar field).

The solar thermal efficiency can be based on either DNI or aperture normal insolation (ANI) in the denominator, though the latter is preferred from a physical standpoint. The thermal efficiency based on ANI is calculated from

$$\eta_{measured} = \frac{P_{measured}}{DNI \cdot \cos\theta \cdot A_{aperture}} \qquad (2)$$

where $\boldsymbol{\eta_{measured}}$ is the thermal efficiency, ANI is the vector of direct normal insolation normal to the trough aperture, $\mathbf{A_{aperture}}$ is the solar field aperture area in tracking mode during the test period, and θ is the solar incidence angle associated with data collected during a test run.

Test Uncertainty: Ascertaining the test uncertainty around the measured power and efficiency is an important element within any solar field acceptance test and has been described in detail in [1, 2]. The ASME in particular has placed critical importance on test uncertainty analyses of all measurements and calculations associated with performance test codes and the Guidelines have drawn heavily on the test uncertainty methodology required for all ASME performance test codes [3].

The expression for the standard measurement uncertainty of a calculated result, $\boldsymbol{u_R}$, based on multiple error sources can in many cases be calculated from the root-sum-square of the total uncertainty of the individual systematic and random uncertainties of a result $\mathbf{b_R}$ and $\mathbf{S_R}$ respectively.

$$u_R = \left[(b_R)^2 + (S_R)^2\right]^{1/2} \qquad (3)$$

where $\mathrm{b_R}$ is the systematic standard uncertainty of a result and $\mathrm{S_R}$ is the random standard uncertainty of a result as calculated by the following equations for $\mathrm{b_R}$ and $\mathrm{S_R}$ where the function R is defined as above for power or efficiency.

$$b_R = \left[\sum_{i=1}^{I}\left(\frac{\partial R}{\partial \bar{X}_i} b_{\overline{X_i}}\right)^2\right]^{1/2} \text{ and } S_R = \left[\sum_{i=1}^{I}\left(\frac{\partial R}{\partial \bar{X}_i} s_{\overline{X_i}}\right)^2\right]^{1/2} \qquad (4)$$

For the equations above, $\mathrm{b_{\bar{X}}}$ is defined as the systematic standard uncertainty of a component and $\mathrm{s_{\bar{X}}}$ is the random standard uncertainty of the mean of N measurements [4]. It is important to note that the "standard" uncertainties described above imply that the calculated result will capture the true result within a 68%

confidence level (one standard deviation). Typically a confidence level of 95% (two standard deviations) is desired by the performance test engineer. For this case, the expanded uncertainty in the result is given by

$$U_{R,95} = 2u_R \quad (5)$$

Tables 1 and 2 below provide a summary of results derived a pretest uncertainty analysis for the power delivered from a "typical" parabolic trough solar field. Similar tables generated for solar field efficiency calculations are provided in the guidelines [1] where the methodology used for the pre-test analysis is described in detail. A similar pre-test analysis would be undertaken with specific instrumentation proposed or selected for the system under test. However, the systematic and random uncertainties of measurement parameters given below are representative of what may occur in a typical field installation. Note that the systematic uncertainty dominates the result, providing 99.6% of the total uncertainty. With respect to the individual contributors, all are of the same order with the HTF specific heat contributing approximately 34% of the total and each of the others about 22%.

Table 1. Table of Data – Solar Field Power

Independent Parameters										
Parameter Information (in Parameter Units)									Uncertainty Contribution of Parameters to the Result (in Results Units Squared)	
Symbol	Description	Units	Nominal Value	Standard Deviation	N_i	Absolute Systematic Standard Uncertainty $b_{\bar{X}_i}$	Absolute Random Standard Uncertainty $s_{\bar{X}_i}$	Absolute Sensitivity $\frac{\partial R}{\partial \bar{X}_i}$	Absolute Systematic Standard Uncertainty Contribution $\left[\frac{\partial R}{\partial \bar{X}_i} b_{\bar{X}_i}\right]^2$	Absolute Random Standard Uncertainty Contribution $\left[\frac{\partial R}{\partial \bar{X}_i} s_{\bar{X}_i}\right]^2$
m	Mass flow rate	kg/s	1200	3.5	180	12	0.3	255.4	9395941	4567
Cp	HTF specific heat	kJ/kg-K	2.48	.007	30	0.031	0.0013	1236000.0	14681159	24217
Thxin	Hot HTF temperature	°C	393	1.2	180	1.0	0.09	2976.0	8856576	71065
Thxin	Cold HTF temperature	°C	290	1.1	180	1.0	0.08	2976.0	8856576	59959

Table 2. Summary of Data - Solar Field Power

Symbol	Description	Units	Calculated Value, R	Absolute Systematic Standard Uncertainty, b_R	Absolute Random Standard Uncertainty, S_R	Combined Standard Uncertainty, u_R	Expanded Uncertainty of the Result, $U_{R,95}$	Expanded Uncertainty of the Result, $U_{R,95}$ (%)
P	Solar Field Power	kJ/s	306528	5894	400	5908	**11816**	**3.9%**

3. Stabilized Test Conditions and Thermal Equilibrium

To achieve successful completion of a test run, the variations in the key test parameters should be low enough to contribute only in a minor way to the uncertainty band in the results. The solar system must be in a stable thermal condition and stable test condition prior to testing. This requires stable characteristics in the solar field inlet temperature and outlet temperature. Stability of the inlet and outlet solar field temperature implies that the HTF mass flow is adjusted adequately to accommodate changes in ANI over the course of the short duration test. Once thermal equilibrium and test condition stability have been reached, the criteria for valid test runs are primarily based on the level of uncertainty as described in Section 2 above.

Stability of Test Conditions: Table 3 shows an illustrative set of stabilization criteria for these conditions based on the influence of the variability of the test parameter on the total uncertainty of the test results. The variability described in Table 3 is defined as the standard deviation of the mean of N measurements of a parameter taken of a test run divided by the average value of the parameter over the test run period. Based on the examples provided by Tables 1 and 2, a combination of the allowable variations given in Table 3 will result in a negligible increase in the total uncertainty of the result. Final stabilization criteria for a specific project will be strongly influenced by the design of the solar system and associated instrumentation, and finally determined by the agreements between the testing parties.

Table 3. Example Stabilization Criteria for Short-Duration Steady State Power Tests of a Utility-Scale Parabolic Trough Solar Field

Parameter	Allowable variability over test period $s_{\bar{X}}/\bar{X}$ (%)
HTF volumetric flow rate, m^3/s	0.5%
ANI, W/m^2	0.5%
Solar field inlet temperature	0.2%
Solar field outlet temperature	0.2%

These criteria are to be applied to evaluate test conditions for stability. In general the potential test period for any given day will occur between 9 a.m. and 4 p.m. Observation of data collected from several operating plants indicates that the variability will be much smaller than the values described in Table 3. For example, 5-second ANI data collected over a 15-minute period (180 data points) varied by approximately ± 2.5 W/m^2 from an average value of 960 W/m^2. The related standard deviation of the data was 1.46 W/m^2. For this instance, the variability as defined in Table 4-1 is calculated by dividing the standard deviation of the mean (1.46/√180) by the average ANI value of 960, resulting in a variability of 0.01%.

Thermal Equilibrium: An estimate of the time necessary to establish thermal equilibrium within a typical solar field was derived using NREL's Solar Advisor Model. The model was run using 5-second time steps to capture the impact of transient effects resulting from a sudden change in solar field inlet temperature. Figure 2 describes the result of an analysis in which the error in a 15-minute average measurement of solar field power, caused by non-equilibrium conditions, is estimated based on varying step changes in inlet temperature. In the figure, $Q_{sf,abs}$ is the power (15-minute moving average) absorbed by the solar field less all thermal losses from the receivers, solar field, and header piping. $Q_{sf,del}$ is the average power delivered to the steam generator. If the solar field is not in equilibrium, e.g., the temperatures of the solar field HTF and the piping/insulation are still changing over time, the delivered power will be less than the absorbed power because some of the excess energy is used to heat the solar field HTF and piping.

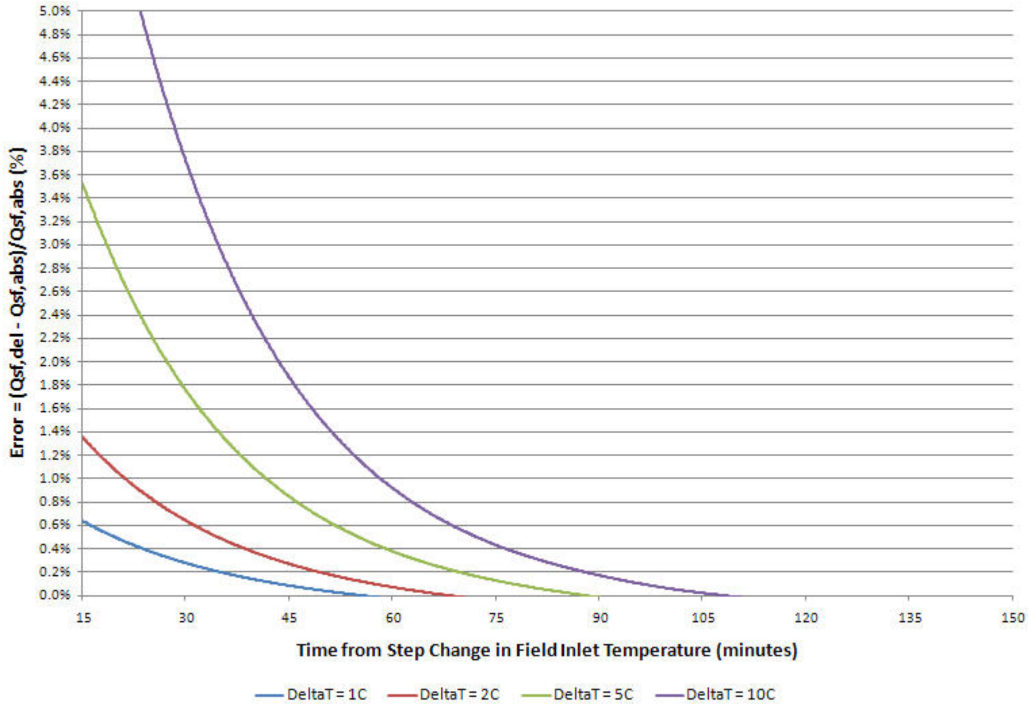

Figure 2. Error Due to Non-equilibrium Resulting from Step Change in Solar Field Inlet Temperature

Using Figure 2 as a guide, we can estimate the time required to minimize the error associated with non-equilibrium conditions to an acceptable level. For example, to limit the error to 0.1% for a 1ºC step change in inlet temperature, approximately 45 minutes is required to establish adequate equilibrium beyond the initial upset, depending on pipe and insulation mass.

4. Additional Uncertainty Considerations Resulting from Changing ANI

Under conditions of a continuously changing ANI, which occurs even during a relatively short-term period, achieving true steady-state conditions is not possible and therefore the impact of varying ANI on an acceptance test must be well understood.

As discussed previously, the solar field acceptance test seeks to compare the measured solar field thermal output to predicted output using a performance model. Consider this relationship as shown in Eqn. 6, where the measured energy on the left as described earlier in Eqn. 1 is compared to the model-projected energy on the right, based on the measured ANI and, in this case, thermal efficiency projected by the model. Any disparity between the left hand side (LHS) and the right had side (RHS) of the equation indicates disagreement between observed and modeled thermal power.

$$\dot{m}\,\bar{C}_p\left(T_{hx,in} - T_{hx,out}\right) = ANI \cdot A_{aperture} \cdot \eta_{thermal,model} \quad (6)$$

The variables in this equation are identical in definition to those defined previously in equations 1 and 2. The percent disparity between instantaneous and observed energy can be expressed as (LHS/RHS – 1) x 100%, and results reported in the following discussion make use of this definition.

Because parabolic trough systems require extensive piping, any energy absorbed within the HTF must often travel long distances before returning to the power cycle. Because changes in ANI levels will not be observed at the outlet of the solar field piping immediately, some time lag is always present between the observed delivered energy and the instantaneous operating conditions. To understand the impact of time lag on transient performance, NREL developed a model that considers the flow of HTF through a representative solar field collector piping system [5]. The NREL model tracks a large number of discrete "plugs" of HTF as they flow through the piping system at a constant velocity. Each plug of HTF interacts thermally with piping and insulation along the flow path, and incorporates a residence time at each calculation node to mimic the actual time delay observed in real piping systems.

Simulation results: The model described above was used to analyze the impact when the ANI slowly increases or decreases over the course of the acceptance test, causing a continual mismatch between the observed delivered thermal power and the modeled incident power. This condition was simulated by applying a gradient to the ANI value once the modeled system reached initial steady-state conditions. To estimate gradients observed during different testing scenarios, we derived representative 30-minute ANI gradients for a summer, spring, and winter day using ANI data collected at NREL's Solar Radiation Research Laboratory located in Golden, Colorado. Figures 3 and 4 show the results of varying the ANI rates for clear days in December and March. In these plots, 'dt' is the length of time variation since the ANI perturbation was applied, and the inset is an expanded view of the period of time after 50 minutes from the start of the simulation.

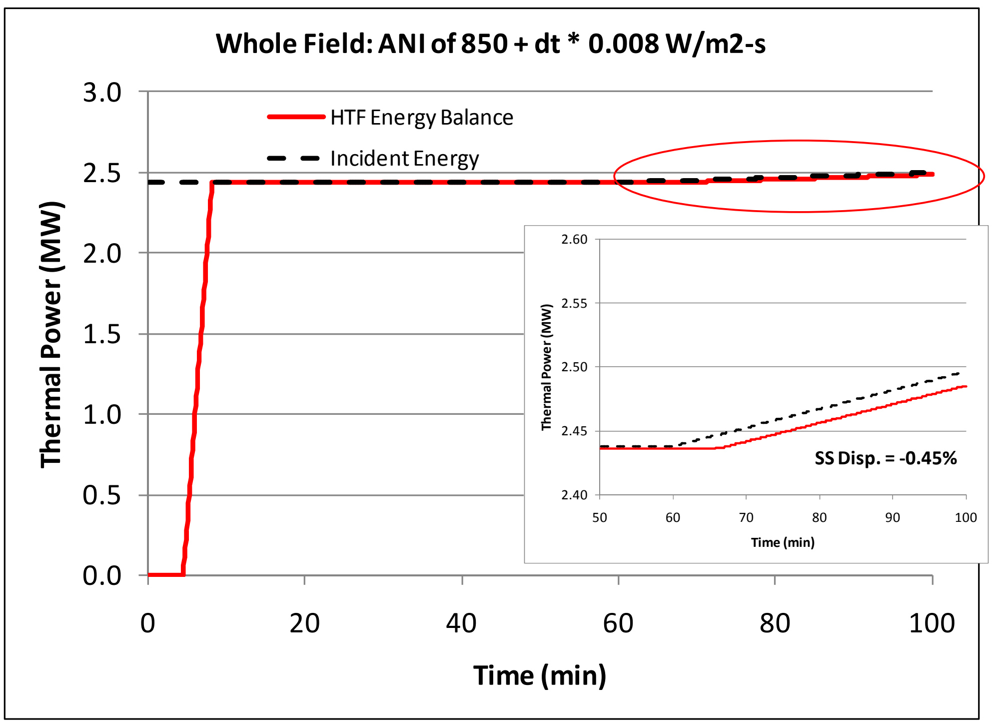

Figure 3. Transient response of a steadily increasing ANI (typical December) in a system with ideal mass flow rate control.

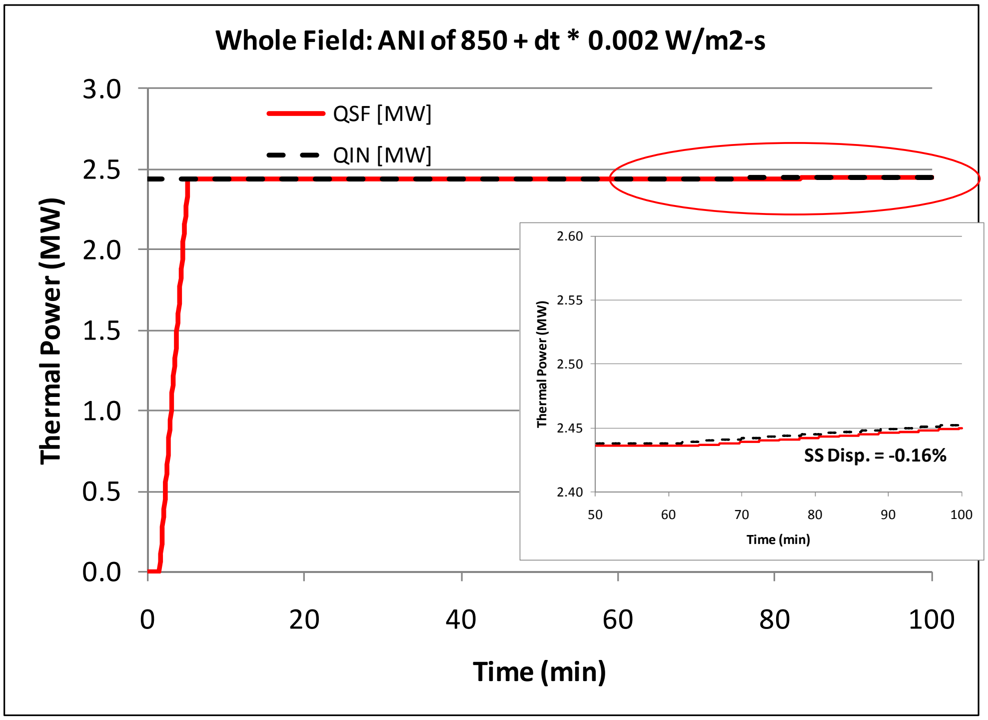

Figure 4. Transient response of a steadily increasing ANI (typical March) in a system with ideal mass flow rate control.

The resulting disparities for each case are presented in Table 4, assuming a system with ideal mass flow rate control to maintain a constant outlet temperature at the solar field exit. For comparison, the ANI gradient that corresponds to a steady-state disparity of 1% is also included. Note that these results are dependent on the base ANI level—850 W/m^2 in this case—and the geometry of the solar field. An increase in the incident thermal energy will cause a corresponding decrease in the steady-state disparity.

Table 4. Summary of Results for Several Representative ANI Gradients

Case Description	Whole field		Subfield	
	Gradient W/m^2-s	Disp. %	Gradient W/m^2-s	Disp. %
March resource profile	0.00214	0.16	0.00214	0.12
June resource profile	0.00743	0.40	0.00743	0.24
December resource profile	0.00848	0.45	0.00848	0.27
1% limiting case	0.02080	1.00	0.03900	1.00

Note that all the errors from the equilibrium effects shown here fall below 0.5%.

One potential pitfall in conducting acceptance testing during off-peak seasons is that the solar resource is typically significantly lower than during the summer months. While the DNI resource is still high in winter, the cosine (Θ) effect reduces the ANI resource considerably. During the January period, the ANI is approximately half of the 850 W/m^2 assumed throughout the analysis presented above. A reduced thermal resource results in a reduced field flow rate, and all transient effects are correspondingly drawn out.

5. Conclusion

Criteria have been discussed and analyzed to assure thermal equilibrium and steady state conditions within the solar field during performance acceptance testing for stability of test conditions (specifically the HTF flow rate, the ANI solar resource, and solar field inlet and outlet temperatures), for sufficient pre-test time durations, and for changes in the solar resource during testing. In each condition, for a representative case example criteria are provided that are achievable in practice and should result in acceptably low uncertainty values or low test errors. For a given site or project, it is recommended that the testing parties examine these conditions through pre-test analyses using specific project parameters, and agree upon acceptable stabilization criteria in a detailed test plan developed prior to the testing period.

Acknowledgements

This work was supported by the U.S. Department of Energy under Contract No. DE-AC36-08-GO28308 with the National Renewable Energy Laboratory.

References

[1] D. Kearney, "Utility-Scale Parabolic Trough Solar Systems – Performance Acceptance Test Guidelines," NREL Report No. SR-5500-48895, http://www.nrel.gov/docs/fy11osti/48895.pdf, May, 2011.

[2] Kearney, D., Mehos, M., (2010), Development of Performance Acceptance Test Guidelines for Large Commercial Scale Parabolic Trough Solar Fields, SolarPACES 2010 Symposium, Sep. 21–24, 2010, Perpignan, France.

[3] ASME PTC 19.1 - 2005 Test Uncertainty.

[4] R.H. Dieck, "Measurements Uncertainty, Methods and Applications," Fourth Edition, ISA, 2007.

[5] Wagner, M., Mehos, M., Kearney, D., McMahan, D., "Modeling of a Parabolic Trough Solar Field for Acceptance Testing: A Case Study" , Proceedings of ASME 2011 5th International Conference on Energy Sustainability & 9th Fuel Cell Science, Engineering, and Technology Conference, Aug. 7-10, 2011, Washington D.C.